11th ANKARA INTERNATIONAL AEROSPACE CONFERENCE **AIAC-2021-1017**
8-10 September 2021 - METU, Ankara TURKEY

INVESTIGATION OF THE AERODYNAMIC HEATING OF A MISSILE USING COMPUTATIONAL FLUID DYNAMICS AND CONJUGATE HEAT TRANSFER METHODS

Beyza Gulcan[1] and Burak Cenik[2]
TOBB University of Economics and Technology
Ankara, Turkey

Sitki Uslu[3]
TOBB University of Economics and Technology
Ankara, Turkey

ABSTRACT

Computational Fluid Dynamics and Conjugate Heat Transfer (CFD-CHT) simulations of a 15o cone-cylinder-flare configuration that analytically and experimentally investigated at NACA in 1958 are performed in order to examine the aerodynamic heating estimation of high-speed missiles (up to Mach 5) and temperature rise that occurs in the electronic devices inside the missile. Time-dependent flight velocity, altitude and angle of attack of the missile were used as table inputs for CFD-CHT analyzes. In simulations, air properties change depending on temperature and ideal gas equation has been utilized. Material properties of solid surface of the missile were also used depending on the temperature. In the comparisons, the temperature data that is used was measured inside the body and was sent to the ground station with a telemeter. After examining the effects of time step, mesh resolution and turbulence model in the analyzes performed as 2D URANS.

INTRODUCTION

In aircraft moving at high speeds, the kinetic energy of the flow around the body transforms into thermal energy as a result of compression and friction [Anderson, 2006]. In approaching some engineering problems, viscous forces can be neglected. However, in cases where the flow velocity is high enough, it is important to include the heating due to viscosity into the calculations when examining the problems. Aerodynamic heating increases with increasing vehicle or flow velocity and becomes even more significant at supersonic speeds. In today's technologies, it is important to consider aerodynamic heating calculations in situations such as supersonic, hypersonic and re-entry. Experiments for these problems are often not feasible or are too difficult or expensive to perform. Therefore, CFD applications play an important role in investigating these types of problems. Considering the mission profile of a missile or a supersonic vehicle, the temperature variation is over a very wide range. For this reason, temperature dependent thermophysical properties of the fluid and the materials used should also be included in the calculations [Sundén, 2017; Fu, 2017]. Increased temperature as a result of aerodynamic heating compromises the structural stability of the missile, and also the temperature rise inside the missile increases the risk of malfunction of avionic unit components.

[1] M.Sc. Student in Department of Micro- and Nano-Technology, Email: bgulcan@etu.edu.tr
[2] Ph.D. Student in Department of Mechanical Engineering, Email: bcenik@etu.edu.tr
[3] Asst. Prof. in Department of Mechanical Engineering, Email: suslu@etu.edu.tr

Many researchers have developed computational methods for aerodynamic heating, such as the reference enthalpy method used by Eckert to estimate the heat transfer rate [Eckert,1960]. The analytical methods established for aerodynamic heating depend largely on the heat transfer rate. However, the heat transfer rate varies according to flight conditions. Therefore, they need validation data for reliable results [Charubhun, 2017]. Computational fluid dynamics analyzes for the thermal analysis of the environment inside the missile are more useful in terms of creating a less costly and easy to control simulation compared to experimental studies. CFD analysis provides highly accurate results for viscous-turbulent and high temperatures using Navier-Stokes equations [Lango, 2004].

The factors affecting the aerodynamic heating have been addressed in various studies. One of the studies on the subject has analyzed the effect of the Mach number and the distance of the first cell of the computational mesh to the wall on the aerodynamic heating [Simsek, 2019]. In another study, static pressure has been modelled in order to investigate the effects of the Stanton number and shear stress on the heat transfer at the surface [Wei, 2018; Rui-Rui, 2018]. In a study conducted with the same test data and missile model some important parameters such as angle of attack and transition regime have been neglected. Moreover, in the said study, the scale of flow models and the created mesh that have been used are not enough for a missile of this length and speed [Charubhun, 2017]. Specifically transitional regime must be considered. In some cases where the flow is turbulent, the boundary layer may switch from laminar to turbulent flow, as well as from turbulent flow to laminar flow. This situation can be called re-laminarization. The state of the boundary layer is an important factor that needs to be examined and resolved as it affects transport phenomena such as surface friction and heat transfer [Bader, 2018]. Narasimha and Sreenivasan studied the re-laminarization process resulting from acceleration. They also carried out a study on other mechanisms that trigger re-laminarization. They mentioned that the re-laminarization process resulting from acceleration is highly cascade and asymptotic, so a completely laminar flow cannot be achieved. This behavior is due to compressive forces that predominate over Reynolds stresses that reacted slowly in a turbulent flow [Narasimha, 1979; Sreenivasan, 1979]. In the NACA report [Charles, 1958; Rumsey, 1958; Dorothy, 1958] it was stated that re-laminarization occurred after the 20th second of the flight. The parameters affecting the flow around the missile can be controlled by Star CCM+. Creating a suitable simulation for supersonic aircrafts by considering all parameters will be worth the time spent since it will be less costly and easier to create than test flights.

The main goal of this research is to foresee the aerodynamic heating of the surface of the supersonic aircrafts using Computational Fluid Dynamics and Conjugate Heat Transfer methods. Parameters such as flow models, transition regime effect is examined by using the Star CCM+. Missile flight test data and missile geometry that have been created by NACA will be used for verification [Charles, 1958; Rumsey, 1958; Dorothy, 1958]

METHOD

Numerical Method

In this study, two dimensional CFD simulations of aerodynamic heating on a conical tipped cylinder missile performed with Unsteady Reynolds Averaged Navier Stokes (URANS) method. For all simulations, implicit unstable solver is used, whose primary function is to check for update at every physical time for computation.

In the simulations, k-w SST was used as the turbulence model. For transition study, the Gamma ReTheta transition model used which is a two-equation, correlation-based transition model that provides a semi-local approach to predict the onset of transition in a turbulent boundary layer. While the 2nd order coupled solver was used to solve the flow domain, 1st order and 2nd discretization to see the effect on the accuracy of the results. 10^{-3} s and 10^{-4} s time steps and 10 inner iterations at each time step were used to solve for the time domain. Also, in the 700K directed mesh model, 10 and 20 internal iteration differences were observed at 10^{-3} s time steps.

The conservation equations for continuity (equation 1), momentum (equation 2), energy (equation 3), are solved in a coupled form, that is, solved simultaneously as an equation vector with the coupled solver. The velocity field is extracted from the momentum equations. Pressure is calculated from the continuity equation and the density is derived from the equation of state.

$$\frac{\partial(\rho E)}{\partial t} + \nabla.(\rho E \upsilon) = f_b.\upsilon + \nabla.(\upsilon.\sigma) - \nabla.q + S_E \tag{1}$$

$$\frac{\partial}{\partial t}\int_V \rho.dV + \oint_A \rho\, \upsilon \otimes \nu.da = -\oint_A pI.da + \oint_A T.da + \int_V f_b\, dV + \int_V S_u dV \tag{2}$$

$$\frac{\partial}{\partial t}\int_V \rho E.dV + \oint_A \rho\, H\, \upsilon \otimes \nu.da = -\oint_A q.da + \oint_A T\, \upsilon.da + \int_V f_b\, .\upsilon dV + \int_V S_u dV \tag{3}$$

Where; t is time, V is volume, a is the area vector, ρ is the density, υ is the velocity, S_u is a user-specified source term, p is pressure, T is the viscous stress tensor, f_b is the resultant of body forces, E is the total energy, H is the total enthalpy, q is the heat flux.

URANS turbulence models present closure relations for the Reynolds-Averaged Navier-Stokes equations, that govern the transport of the mean flow quantities. Each solution variable Φ in the instantaneous Navier-Stokes equations is seperated into its mean value and its fluctuating part in order to obtain the Reynolds-Averaged Navier-Stokes equations [Siemens, 2021].

$$\phi = \overline{\phi} + \phi' \tag{4}$$

Φ stands for velocity components, pressure, energy, or species concentration. The averaging Navier-Stokes equation transform might be supposed of as time-averaging for steady-state situations and ensemble averaging for repeatable transient situations. The mean mass, momentum, and energy equations can be written as:

$$\frac{\partial \rho}{\partial t} + \nabla.(\rho\overline{\upsilon})0 \tag{5}$$

$$\frac{\partial}{\partial t}(\rho\overline{\upsilon}) + \nabla.(\rho\overline{\upsilon}\ \otimes \overline{\nu}) = -\nabla.\overline{p}\ I + \nabla.(\overline{T} + T_{RANS}) + f_b \tag{6}$$

$$\frac{\partial}{\partial t}\left(\rho\overline{E}\right) + \nabla.\left(\rho\overline{E}\overline{\upsilon}\right) = -\nabla.\overline{p}.\bar{\upsilon} + \nabla.\left(\overline{T} + T_{RANS}\right)\bar{\upsilon} - \nabla.\overline{q} + f_b\overline{\upsilon} \tag{7}$$

Where; ρ is the density,υ is the mean velocity, p is the mean pressure, I is the identity tensor, T is the meean viscous stress tensor, f_b is the resultant of the body forces (such as gravity), E is the mean total energy per unit mass, q is the mean heat flux.

In fact, these equations are basically the same as the Navier-Stokes equations. However, an additional term arises here in the momentum and energy transport equations. This term is the stress tensor and is expressed as follows:

$$T_{RANS} = -\rho\begin{pmatrix}\overline{u'u'} & \overline{u'v'} & \overline{u'w'}\\ \overline{u'v'} & \overline{v'v'} & \overline{v'w'}\\ \overline{u'w'} & \overline{v'w'} & \overline{w'w'}\end{pmatrix} + \frac{2}{3}\rho kI \tag{8}$$

Where k is the turbulent kinetic energy.

Therefore, it is difficult to model the RANS according to the mean flow variables since obtain closure of the governing equations.
In the scope of the study, k-w SST and k-w gamma-ReTheta transition models were used to model the turbulent flow. The k-w turbulence model is a two-equation model that solves two transport equations for '*k*' and '*w*' variables to calculate turbulent eddy viscosity. Where *k* is the kinetic energy of turbulence, and *w* is the specific dissipation rate.

For this problem, he proposed the 'ω' transport equation instead of the 'ε' transport equation in the standard k-epsilon model.

The k-ω model has a similar structure to the k-ε model, but there is an additional non-conservative cross-diffusion term here. This term includes a dot product of k and ω '(∇k.∇ω)'. Menter mentioned a blending function. This function changes according to the distance from the wall. It uses a ω -weighted blending function near the wall and an ε-weighted blending function away from the wall.

RESULTS AND DISCUSSIONS

Validation and Mesh Independency

An 86-inch missile with a 15-degree conical nose and a 10-degree tail angle has been used for the test flight. The missile surface has been coated with an 0,03-inch Inconel. 23 thermocouples have been placed inside the interior wall of the missile in order to measure the aerodynamic heating of the surface. The maximum Mach number achieved during the flight has been measured as 4.2 The altitude reached after 26 seconds of flight has been measured as 60000 ft. In order to ease the mesh in the model created for the analyzes, the missile have been divided in half from the x axis and the bottom line has been considered axisymmetric boundary condition. The material density of the coating material Inconel x-750 has been used as a constant. Heat transfer coefficient and specific heat values are entered as polynomials. The Mach numbers taken from the test flights have been plotted and the obtained equation has been entered into the solver as a field function. In Figure 1, a drawing of the missile and thermocouple stations are shown.

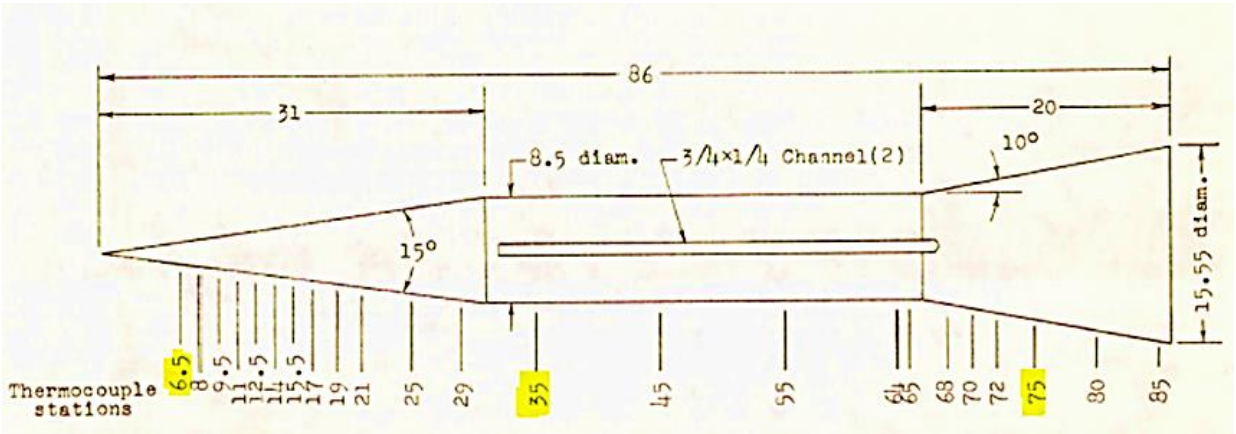

Figure 1: A drawing of the missile and thermocouple stations [Charles, 1958; Rumsey, 1958; Dorothy, 1958].

In this study, the results from the nose, cylinder and flare part at one each point were compared with the results of CFD-CHT calculations. Station measurements at 6.5 inches for the nose section, 35 inches for the cylinder section and 75 inches for the flare section were used.

Time dependent altitude and Mach values are used as free stream boundary conditions. Altitude and Mach number variation with time are given in Figure 2.

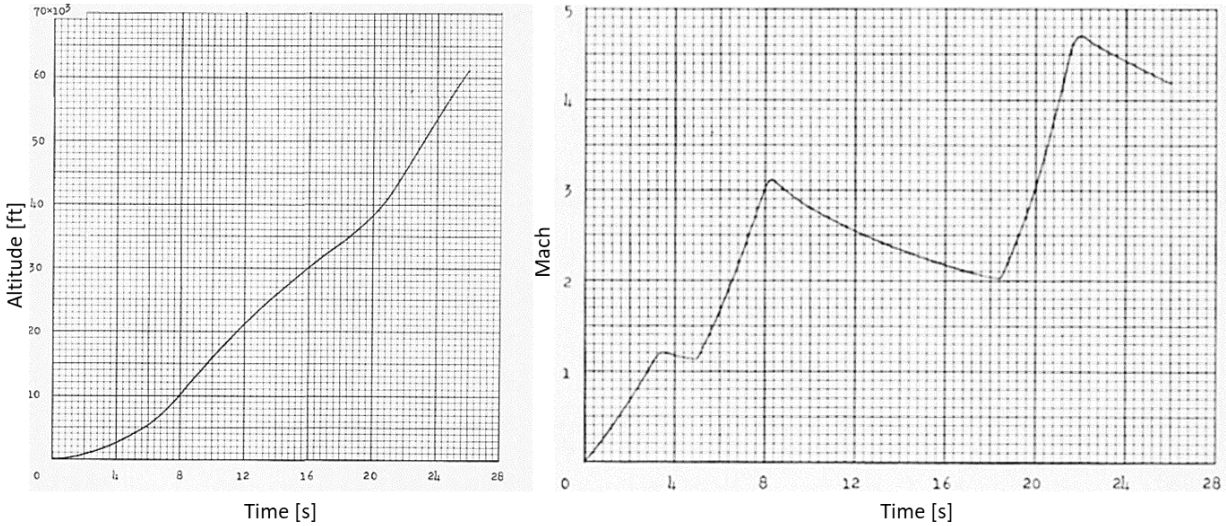

Figure 2: The Variation of Altitude and Mach Number with time [Charles, 1958; Rumsey, 1958; Dorothy, 1958].

On the mesh studies performed; 1.8 million cells have been obtained on the polyhedral-type mesh, 250.000 cells and 750.000 cells have been obtained on the directed mesh. These three types of mesh are shown in Figure 3,4 and 5.

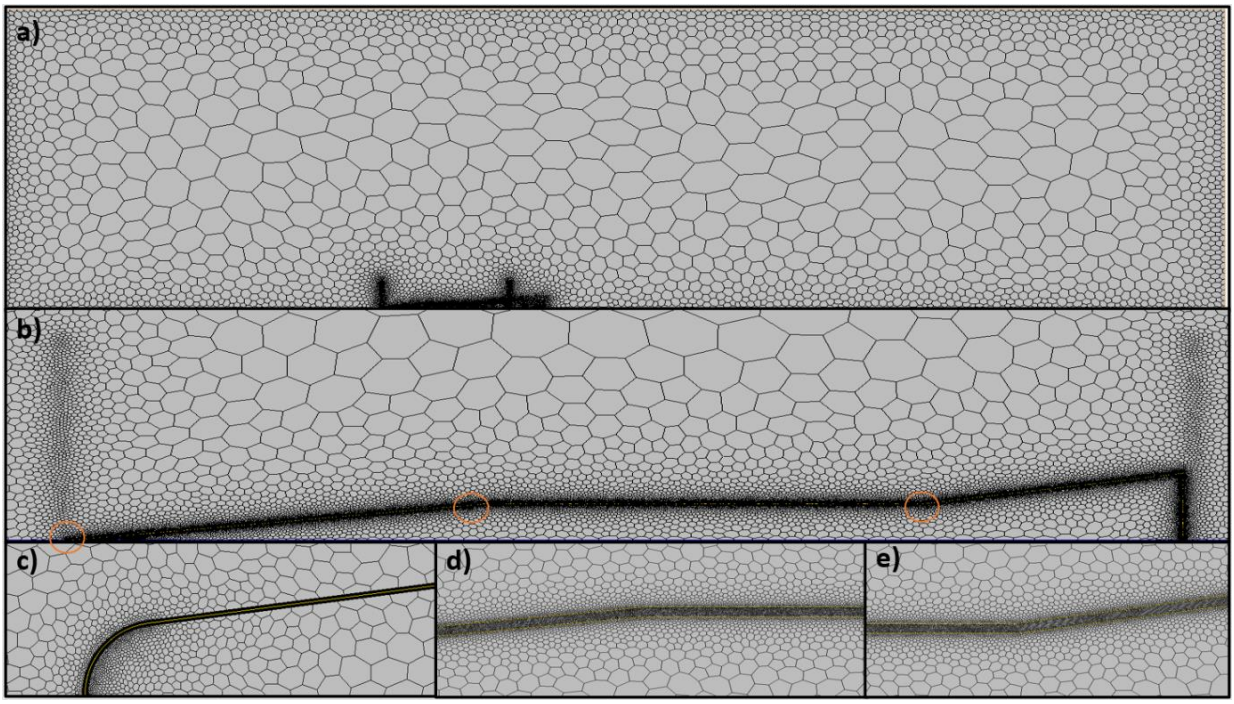

Figure 3: Created solution network with polyhedral mesh (Total mesh number 1.8 million), a) Full domain, b) Close up image, c) Nose section d) Nose-cylinder intersection, e) Cylinder-flare intersection.

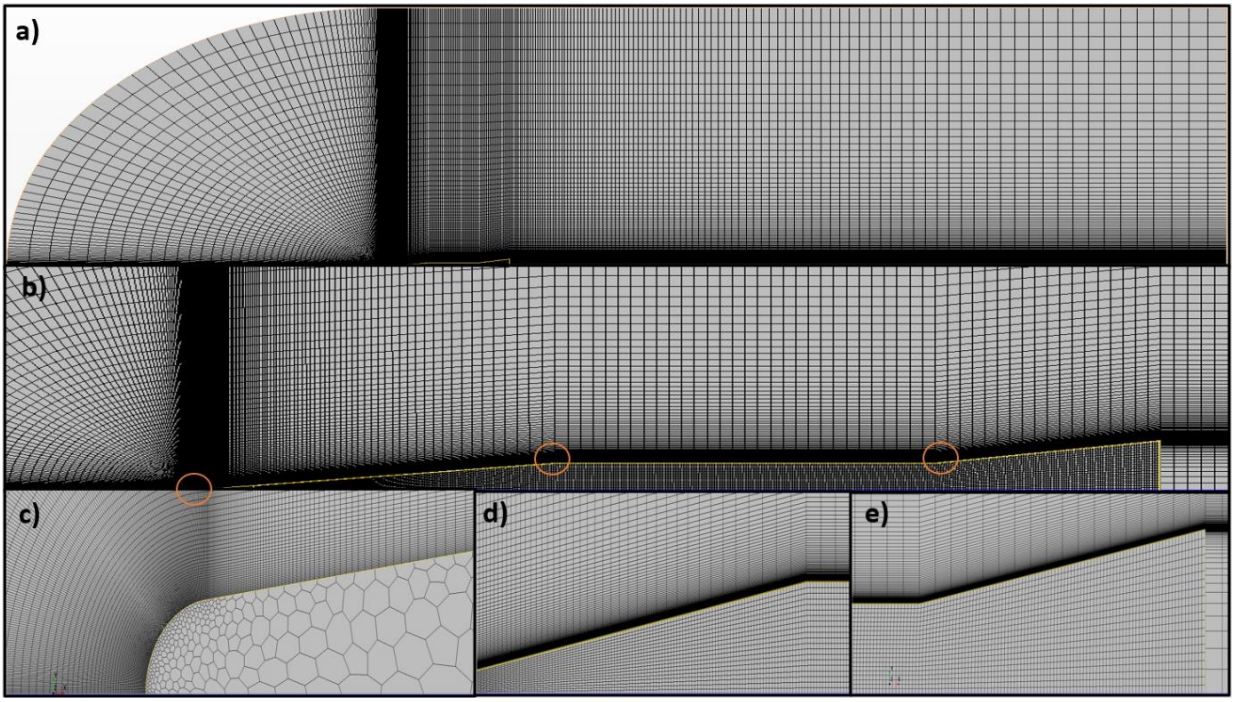

Figure 4: Created solution network with directed mesh (Total mesh number 250 thousand). a) Full domain, b) Close up image, c) Nose section d) Nose-cylinder intersection, e) Cylinder-flare intersection.

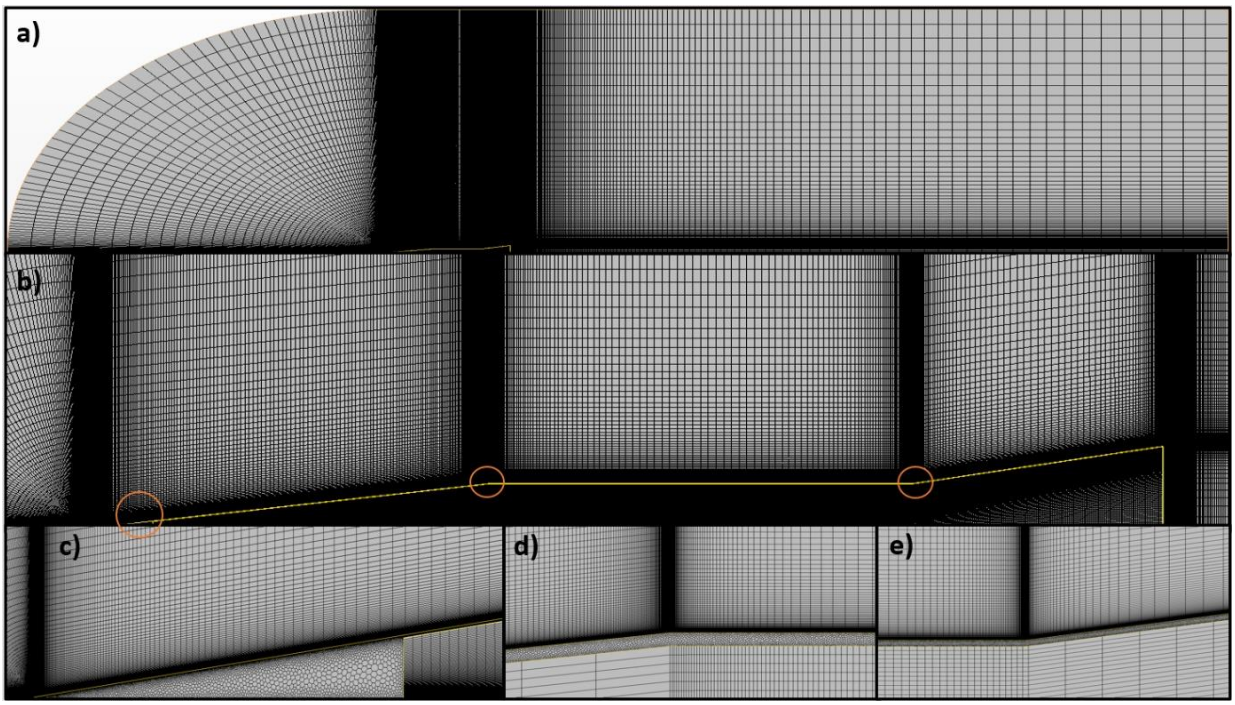

Figure 5: Created solution network with directed mesh (Total mesh number 750 thousand). a) Full domain, b) Close up image, c) Nose section d) Nose-cylinder intersection, e) Cylinder-flare intersection.

Even though the solution mesh obtained via the directed mesh contained less cells, it has been observed that the results of the analysis are more compatible with the test data compared to the polyhedral mesh domain. This situation shows that the CPU cost can be reduced with directed mesh.

The results of CFD-CHT calculations for these three types of computational meshes are given in Figure 6. Test results were compared with the measurements for the nose, cylinder and flare part. Directed mesh gives a more promising result than polyhedral mesh, also considering the CPU cost, and results of two mesh types containing 750,000 and 250,000 cells have almost the same agreement with the experimental data. In addition, directed mesh analyzes containing 2.1 million cells are ongoing and comparison will be made with current mesh studies.

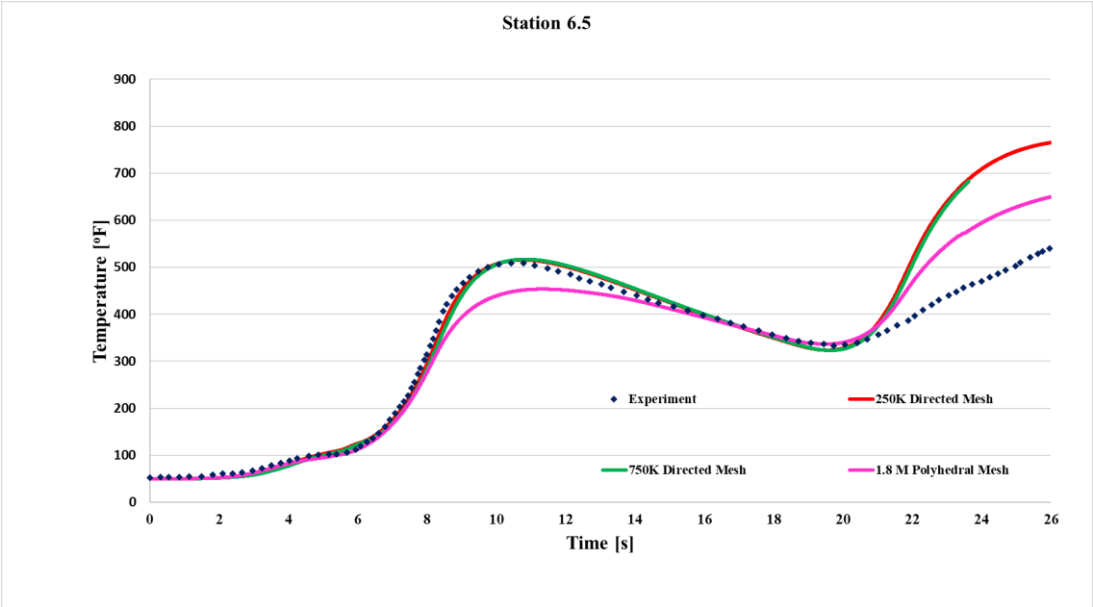

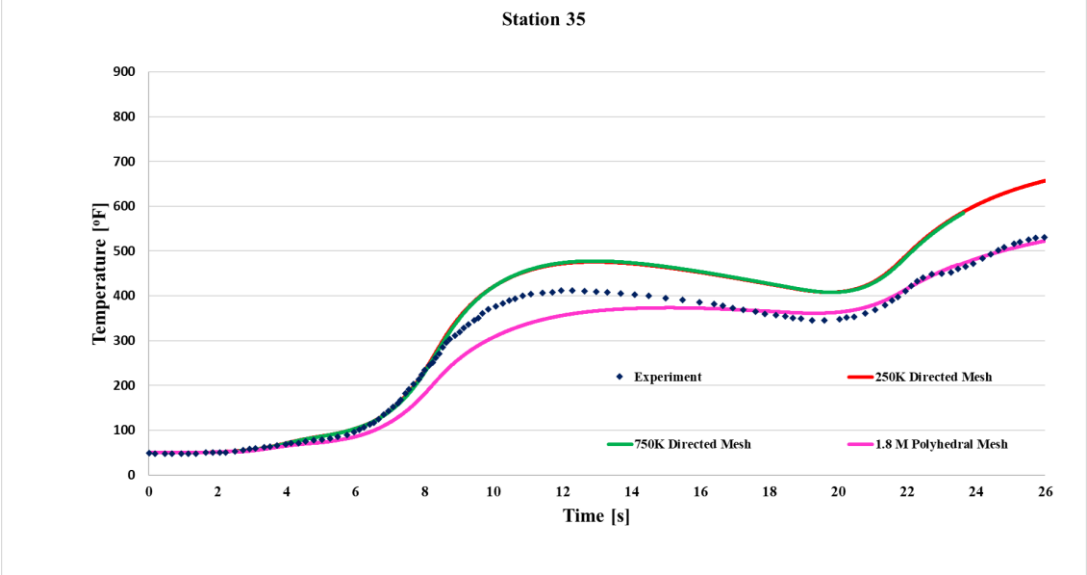

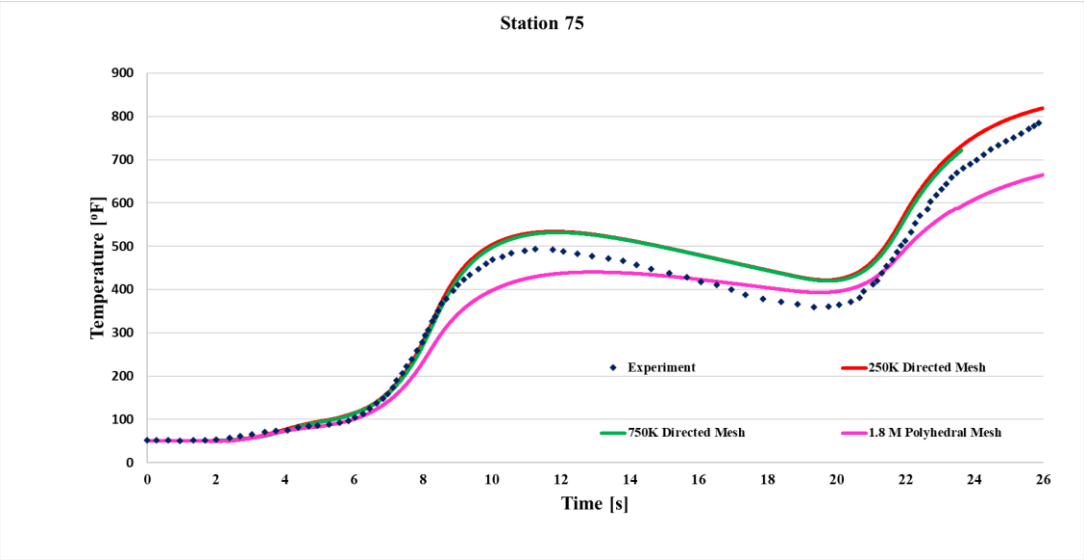

Figure 6: Comparison of experimental data with temperature results obtain from mesh study for respectively nose (6.5), cylinder (35) and flare (75).

Turbulence Models and Time variables

The k-w SST turbulence model generally has promising results for external flow problems and also where the boundary layer is important. For this reason, the k-w SST model from the k-w turbulence model family was used in the studies, and the gamma-ReTheta transition model was used to observe the laminar-turbulence or turbulence-laminar transition. Figure 7 shows the comparison of two different turbulence models with the experimental results.

Figure 7: Comparison of experimental data with temperature results obtain from turbulence study at 250k directed mesh for respectively nose (6.5), cylinder (35) and flare (75).

According to the results of the first analysis, a suitable agreement has been achieved for the cylinder and the flare in the results obtained with 10^{-3} s time step. Smaller time step (10^{-4} s) is also performed. Nonetheless, the temperatures obtained from the analysis performed after the 18. second on the nose, have been calculated much higher than the experimental data. The effect of two different time step values on the results is shown in Figure 8.

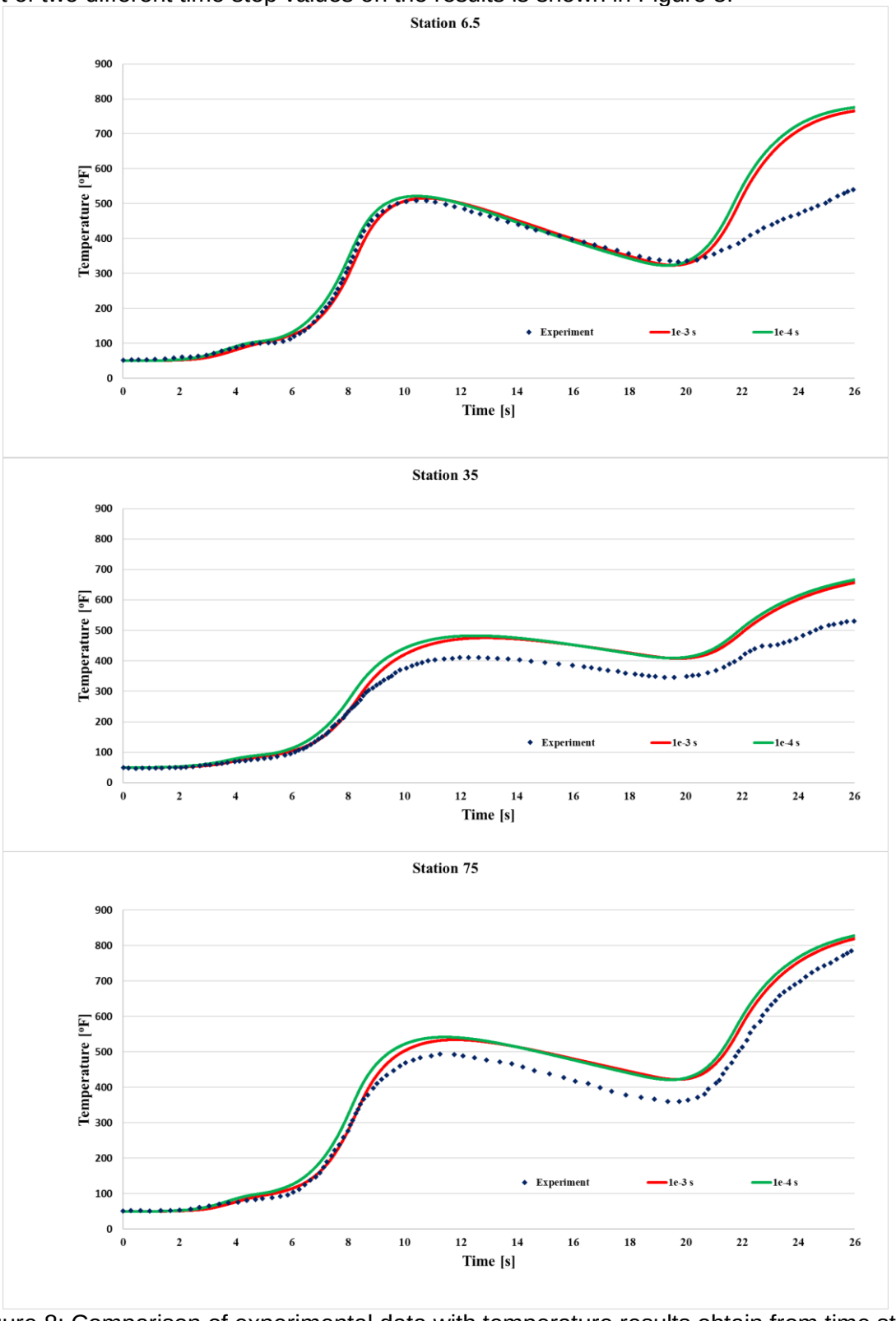

Figure 8: Comparison of experimental data with temperature results obtain from time step study at 250k directed mesh for respectively nose (6.5), cylinder (35) and flare (75).

As a result of the analyzes performed for two different time steps (10^{-3} s and 10^{-4} s), the same results with the experiment were obtained. Compared to the experiment on the nose part, a smaller time step value did not solve the high temperature prediction problem. Therefore, all other analyzes were performed with a time step of 10-3s.
In addition, the effect of 2nd order temporal discretization on the calculations was examined and shown in Figure 9.

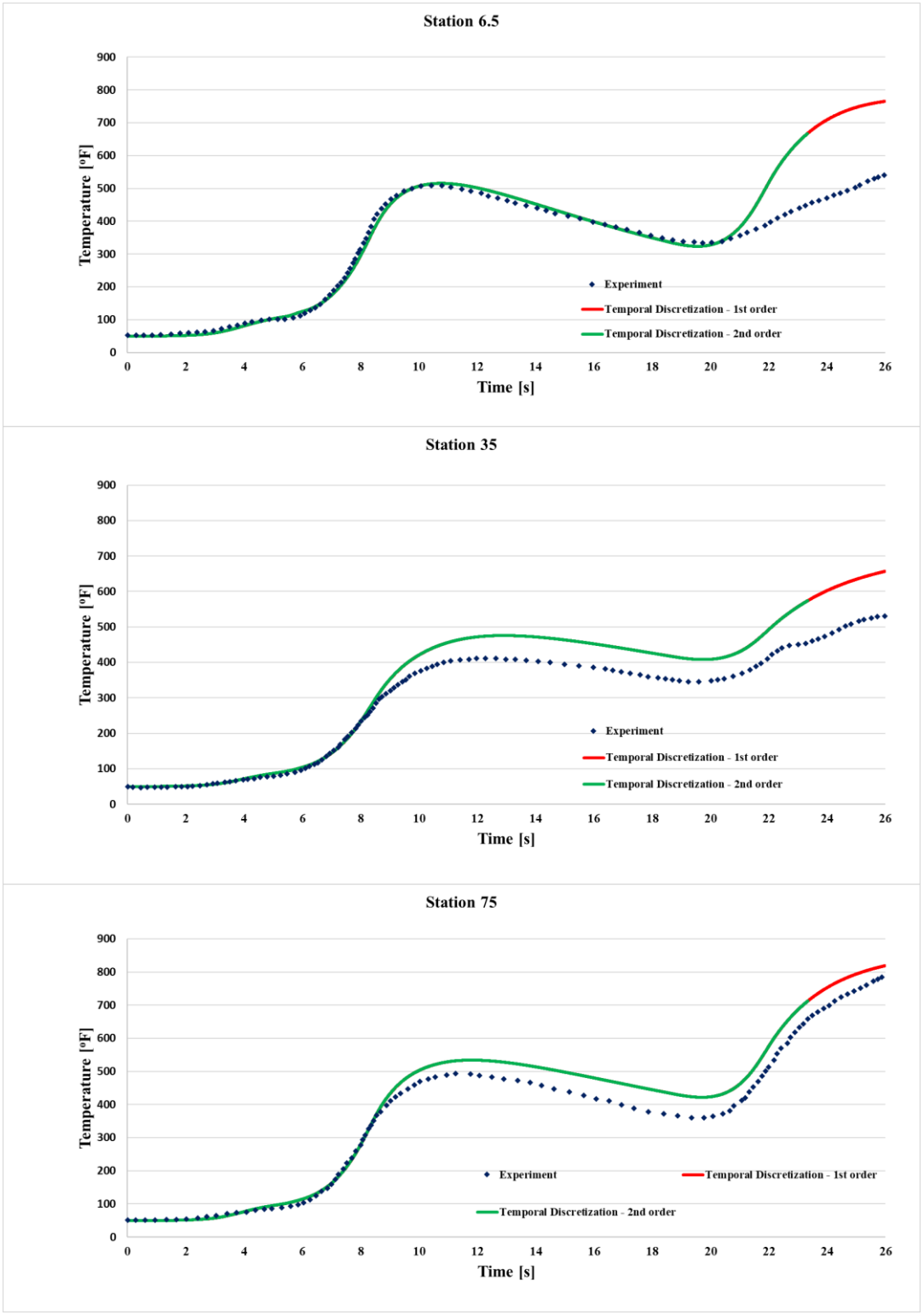

Figure 9: Comparison of experimental data with temperature results obtain from time order study at 250k directed mesh for respectively nose (6.5), cylinder (35) and flare (75).

The number of iterations performed in a time step is called inner iteration. Ten inner iterations were used in the studies. When Figure 2 is examined, the Mach profile increases very abruptly after 18s. For this reason, the effects of the inner iteration number on the solution were investigated in order to catch the change here.

Figure 10: Comparison of experimental data with temperature results obtain from inner iteration study at 750k directed mesh for respectively nose (6.5), cylinder (35) and flare (75).

The results inner iteration study are examined in detail in the Discussion section given in Figure 10.

Instead of the Gamma-ReTheta transition model, which was used until the 18s, to solve the laminarization zone that occurred around the 20s in the nose section, a laminar approach was adopted after 18s. The results of this study are given in Figure 11. In all 3 sections, temperatures were calculated less than the experiment after 18s. All the studies have been examined in detail in the Discussion section.

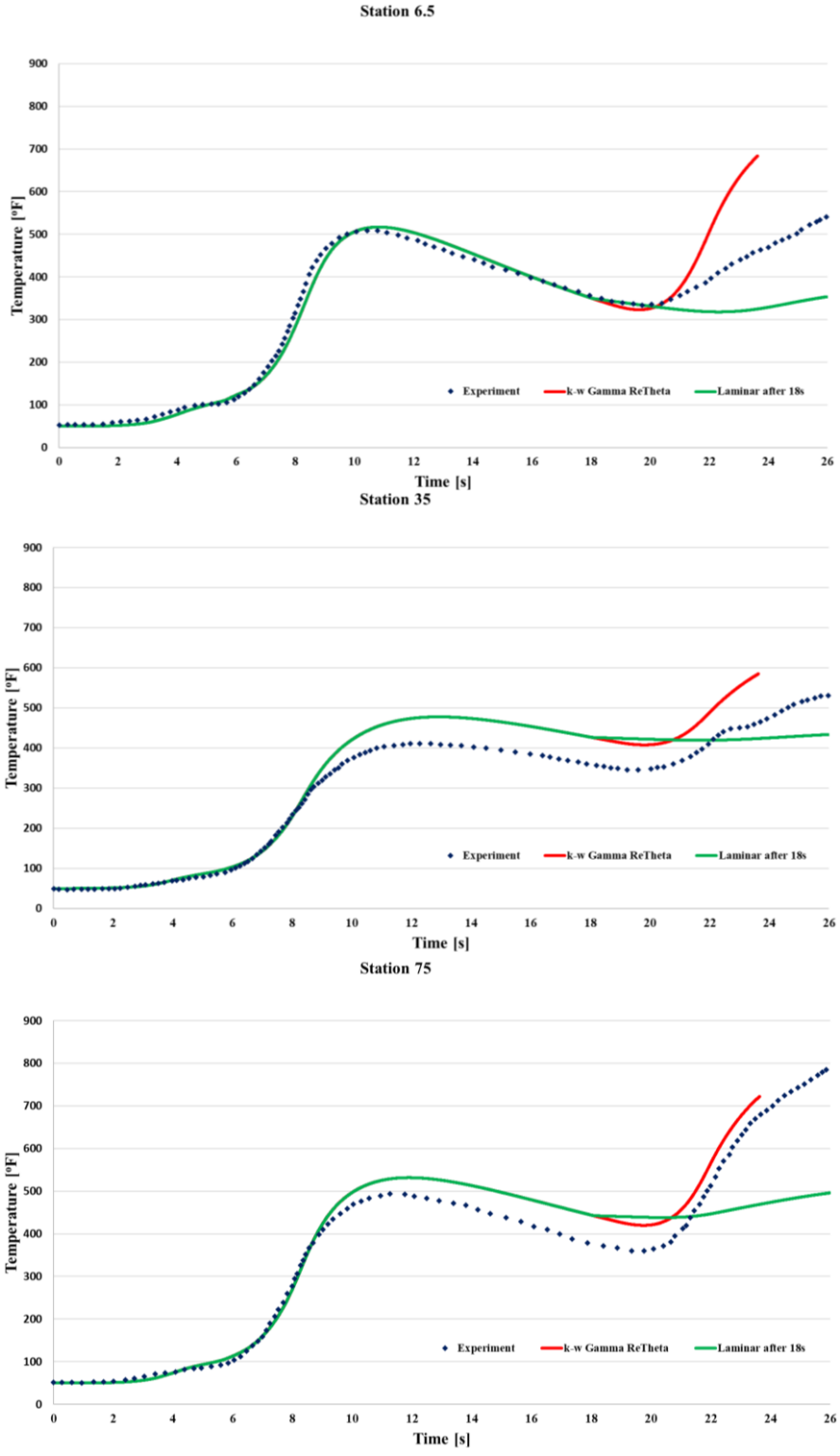

Figure 11: Comparison of experimental data with temperature results obtain from flow regime study at 750k directed mesh for respectively nose (6.5), cylinder (35) and flare (75).

Discussion

In this study, 2D CFD-CHT URANS analyzes of a 15^o Cone-Cylinder-Flare configuration missile were performed and compared with the test results in the literature. Although the 3D effect was not examined and the URANS approach was used, promising results were obtained when compared with the experiment. In all studies, different results than experiment (up to 250 K) were obtained in the nose section after the 20 s.

When the results of the two turbulence models were compared with the experimental results, no difference was observed between the approaches. While both models are in good agreement with the experiment up to the 20 s in the nose section, both of the two turbulence models predict higher temperatures after the 20 s than in the experiment. After 20 s, the difference between the experiment and the calculations reaches 250 K values. This was not observed for the Cylinder and Flare sections and were generally in good agreement with the experiment. 3D effects are excluded from the scope of the study. With a 3D computational domain, better results can be obtained in the cylinder and flare parts than the current results. However, this estimate for the nose part will not be very realistic. The difference here is thought to be due to the re-laminarization of the flow after the 20 s in the nose section. While the transition model can solve the transition from laminar to turbulent, it cannot solve the opposite situation. For this reason, a transition model that can calculate the transition from turbulence to laminar should be used in order to eliminate this discrepancy in the nose.

The effects of time step and temporal discretization were examined and no difference was observed for this problem. Furthermore, the effects of the number of iterations in a time step (inner iterations) on the solution were investigated. As the number of inner iterations increased, the temperature difference between the experiment and the calculations decreased after 20 seconds. For this reason, 30 inner iteration case is currently under investigation and the results have not been obtained yet. It is estimated that with the turbulence model that will catch the transition from turbulence to laminar mentioned above and the high inner iteration number will eliminate the deviation occurring after 20 seconds. The Mach profile applied in boundary conditions around 20s increases very sharply and rapidly. Therefore, an increase in residual values has been observed since this time. By increasing the inner iteration value around 18-20s, the numerical instability problem caused by the sudden change here can be prevented.

As a result of the analyzes carried out by making the assumption of full laminar flow after 18 s, lower temperatures were calculated in the nose section after 18 s compared to the experiment. In addition, discrepancies from the experiment also occurred in the cylinder and flare section. After this period, the flow does not completely switch to a fully laminar state. For this reason, this approach does not perform correct results and it has been observed that a transition model or correlation is needed again.

In general, the calculations are in good agreement with the experimental data, except for the after 20s in the nose section. Analyzes currently in progress will be completed and compared with current results for future work. In addition, transition model study to solve the discrepancy occurring after 20s in the nose section and more detailed inner iteration studies will be carried out to solve numerical problems caused by rapid boundary condition change. In addition to these, in order to examine the 3D effect, firstly analyzes can be made on a 30^o sector and then calculations can be made on a 360^o computational domain.

REFERENCES

Anderson, J.D. (1989) Hypersonic and High Temperature Gas Dynamics, Vol 2, p:6-7, McGraw-Hill, Washington, 2006.

Bader, P. (2018) Experimental Investigation of Boundary Layer Relaminarization in Accelerated Flow, Journal of Fluids Engineering, Graz University of Technology, Austria, 2018.

Charles, B. and Dorothy B. (1958) Measurements of Aerodynamıc Heat Transfer on a 150 Cone-Cylınder-Flare Configuratıon in Free Flight at Mach Numbers Up To 4.7, Langley Aeronautical Laboratory Langley Field, Va., 1958.

Charubhun, W. and Chusilp, P. (2017) Aerodynamic Heat Prediction on a 15 degree Cone-Cylinder-Flare Configuration Using 2D Axisymmetric Viscous Transient CFD, Aeronautical Engineering Division Defence Technology Institute Pakkret, Nonthaburi, Thailand, 2017.

Eckert, E.R.G. (1960) Survey of Boundary Layer Heat Transfer at High Velocities and High Temperatures, WADC Tech, p: 59-264, WrightPatterson AFB, Ohio, 1960.

Longo, J.M.A. (2004) Modellıng Of Hypersonıc Flow Phenomena, German Aerospace Center (DLR), RTO-EN-AVT-116, 2004.

Narasimha, R. and Sreenivasan, K.R. (1979) Relaminarization of Fluid Flow, Advances in Applied Mechanics, p:221–309, 1979.

Siemens (2021) Simcenter Star-CCM+ Theory Guide. Siemens PLM Software.

Simsek, B. (2019) Aerodinamik Isınmanın ve Isıl Koruma Sistemlerinin Aerodinamik Isınmaya Bağlı Termo-kimyasal Aşınmasının İncelenmesi, Tobb Ekonomi ve Teknoloji Üniversitesi Fen Bilimleri Enstitüsü, Makine Mühendisliği Anabilim Dalı, Doktora Tezi, 2019.

Sunden, B. and Fu, J. (2017) Aerodynamic Heating. p:27–44, Heat Transfer in Aerospace Applications, 2017.

Wei, H. and Rui-Rui, Z. (2018) Numerical Experiment on The Flow Field Properties of a Blunted Body With a Counterflowing Jet in Supersonic Flows, Acta Astronautica, April 2018.